

Molecular-dynamics investigation of the surface stress distribution in a Ge/Si quantum dot superlattice

I. Daruka and A.-L. Barabási

Department of Physics, University of Notre Dame, Notre Dame, Indiana 46556

S. J. Zhou

Applied Theoretical and Computational Physics Division, Los Alamos National Laboratory, Los Alamos, New Mexico 87545

T. C. Germann, P. S. Lomdahl, and A. R. Bishop

Theoretical Division, Los Alamos National Laboratory, Los Alamos, New Mexico 87545

(Received 6 April 1999)

The surface stress distribution in an ordered quantum dot superlattice is investigated using classical molecular dynamics simulations. We find that the surface stress field induced by various numbers (from 1 to 9) of Ge islands embedded in a Si(001) substrate is in good agreement with analytical expressions based on pointlike embedded force dipoles, explaining the tendency of layered arrays to form vertically aligned columns. The short-ranged nature of this stress field implies that only the uppermost layers affect the surface growth and that their influence decreases rapidly with layer depth. [S0163-1829(99)52028-6]

Self-assembled quantum dots are promising candidates for many optoelectronic applications. However, for some advanced devices (e.g., quantum dot lasers) larger island density is also of great importance. One way to achieve this is by depositing multiple layers of quantum dots. In the growth of these quantum dot superlattices, the first layer of dots grown on top of a wetting film is covered by a thin capping layer that ensures a relatively flat terrain to nucleate and grow a second layer of islands. After this second layer is formed on top of a second wetting film (which forms spontaneously in the growth process), a new capping layer is deposited. This process may be repeated several times, finally resulting in a multilayer dot configuration referred to as a quantum dot superlattice (QDSL). While there is no (horizontal) spatial ordering in the first island layer, the islands in the second layer prefer to nucleate above the islands of the first layer. This vertical self-ordering tendency increases as more layers are deposited, leading to vertically aligned columns of islands.

A number of experiments have investigated this process of vertical self-ordering. Most of these have been performed on InAs islands grown on a GaAs substrate (see, e.g., Ref. 1), but other systems have been investigated as well.² More complicated structures have also been fabricated where the dots do not align vertically, but instead follow an fcc-crystal-like stacking sequence with a tunable dot-lattice period.³ These experiments demonstrated that the quality of alignment depends strongly on the capping layer thickness, with thinner capping layers yielding better vertical correlation.¹ It is also observed that in some cases the average island size⁴ and size uniformity⁵ increase with the layer number.

In spite of the great experimental interest, there have only been a few theoretical studies of vertical ordering. One analytic approach⁶ invokes pointlike embedded islands to calculate the stress field on the surface, which determines the preferred nucleation sites for the next island layer. This simple model accounts both for the vertical alignment and for the

increased size uniformity. This and subsequent models⁷ have demonstrated the important role the stress field of the buried islands play in the vertical self-ordering process. Consequently, in order to properly model and understand the formation of QDSLs, we have to be able to properly model the stress field of the buried islands. Most models have relied on continuum elasticity, but there is little information on how well these solutions describe the stress field observed in the crystals formed of discrete atoms. Our goal here is to address this question using molecular dynamics (MD) techniques to investigate how the surface stress is influenced by adding multiple layers of stacked island structures. Due to recent advances in the use of massively parallel computers in large-scale simulation of many million atoms⁸⁻¹⁰ we are now able to model systems with dimensions comparable to experimental ones, and also to take into account symmetry effects of the diamond lattice that were not included in the analytic approach⁶ or in the finite-element calculation.¹ In order to see how well stacked quantum dot systems can be approximated by a system of pointlike dots, we compare our MD results to the analytic solution for the stress distribution of point-like dot systems. We demonstrate that by choosing appropriately the parameters in the force-dipole approximation, these analytic solutions can offer an excellent fit to the stress fields measured in the MD simulations.

We use the three-dimensional (3D) MD code, SPaSM (scalable parallel short range molecular dynamics),^{11,12} designed for very large scale simulations on a variety of parallel computing platforms. Subsequent improvements of SPaSM, including the use of a scripting language, allow one to visualize, filter, and analyze the huge amount of data produced from a simulation of millions of atoms,¹³ perhaps the most challenging problem encountered in large-scale computer simulations.

From the wide range of experimentally studied heteroepitaxial systems in which vertical ordering was observed we choose Ge/Si (Ref. 14) for our investigations. We model

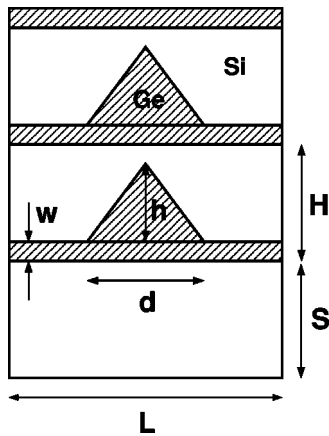


FIG. 1. Schematic of the system geometry used in the MD simulation.

pure Ge islands capped by Si layers on a Si(001) substrate. The geometry of the system is shown in Fig. 1. Pyramidal islands are placed on top of each other, separated by a Si capping layer and a 4-monolayer-thick Ge wetting film. Initially we place all Ge atoms on Si lattice sites, thus starting out with Ge islands compressed by $\sim 4\%$ to match the Si lattice constant. In both directions (x, y) parallel to the surface we apply periodic boundary conditions, while we use free boundary conditions in the (z) direction perpendicular to the surface. We therefore are describing a periodic array of vertically aligned quantum dot columns.

We use the empirical Stillinger-Weber potentials for Si (Ref. 15) and Ge,¹⁶ which include three-body (bond angle) terms in addition to the usual pairwise interactions. While the Stillinger-Weber potential has known difficulties in describing particular surface reconstructions such as the Si(111)(7×7) surface,^{17,18} it is reasonably accurate for the (001) surface¹⁹ and should be particularly reliable for the coherently strained structures close to equilibrium which are considered here. The system is elastically relaxed using a kinetic annealing algorithm in which the velocities of all atoms are set to zero whenever the total kinetic energy of the system reaches a maximum.²⁰ The total potential energy of the system is monitored to determine when this relaxation has converged. This typically takes between two thousand and ten thousand timesteps, corresponding to a few picoseconds of simulation time.

Systems with 1, 2, 3, 6, and 9 dot layers were simulated. Each Ge island has a height of $h = 2.8$ nm and a diameter of $d = 11.2$ nm, corresponding to approximately 5000 atoms per island. The horizontal edge-to-edge spacing between islands was $L = 22.4$ nm, and the vertical spacing between the island layers was $H = 4.5$ nm, including a $w = 4$ monolayer (5.6 Å) Ge wetting film thickness. The underlying Si substrate was $S = 17$ nm thick in all simulations, and the largest simulated system (9 dot layers) included a total of three million atoms.

To calculate the local stress tensor at each atomic site, we use a formulation similar to that derived by Hardy.²¹ Since we are considering an equilibrium structure, the kinetic contribution is zero and may be ignored. For pairwise interactions, the stress tensor elements are computed as

$$S_i^{\alpha\beta} = -\frac{1}{2V_i} \sum_j F_{ij}^{\alpha} r_{ij}^{\beta}, \quad (1)$$

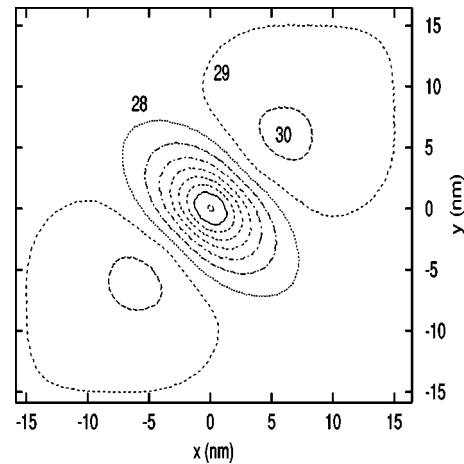


FIG. 2. Contour plot of the surface stress field σ for a single embedded quantum dot layer. Contours are evenly spaced every 10^9 erg/cm³, from 21×10^9 erg/cm³ to 30×10^9 erg/cm³.

where \mathbf{F}_{ij} is the force on atom i due to atom j , \mathbf{r}_{ij} is the internuclear vector, and $\alpha, \beta = x, y, z$ label the Cartesian components. The three-body forces may be similarly included, since each three-body term consists of a pair of interactions between a central vertex atom i and the neighboring atoms j and k . Since Hardy's original formulation is based on a coarse-grained rather than an atomistic resolution of stresses, we are forced to introduce a necessarily arbitrary definition of the "atomic volume" V_i . We take this to be the volume of a sphere with radius equal to the distance to the nearest neighboring atom. This distance varies by less than half of one percent over the surface, so the resulting stress tensor is qualitatively unaffected by the definition chosen for V_i . We found in all cases that the off-diagonal components of the surface stress tensor ($\sigma_{ij}, i \neq j$) and vertical component σ_{zz} were negligible. An example of the surface stress distribution is shown in Fig. 2 as a contour plot of $\sigma = \sigma_{xx} + \sigma_{yy}$ on the surface for a single-layer system.

To investigate the stress contribution of the consecutive dot layers, Fig. 3 shows σ along the (110) [Fig. 3(a)] and the ($1\bar{1}0$) [Fig. 3(b)] directions for various numbers of dot layers. It can be seen in each plot that a prominent minimum occurs directly above the existing vertical column of dots. However, while in the (110) direction there is a local maximum on each side of the minimum, in the ($1\bar{1}0$) direction no local maximum exists. This difference can be understood by recalling that for the diamond lattice the (110) and the ($1\bar{1}0$) directions are not equivalent, a symmetry effect not accounted for in previous theoretical work.^{1,6} Another, more direct, demonstration that the preferential site for subsequent deposition is directly above existing dots is obtained by moving a "probe" Ge atom across the surface, adjusting its height at each point to minimize the total energy (while keeping the rest of the system frozen). This procedure leads to a surface energy profile which is qualitatively indistinguishable from the stress profiles in Figs. 2 and 3, including the local maxima seen along the (110) direction in Fig. 3(a).

Since the stress curves nearly coincide for the 3, 6, and 9 dot layer cases, we conclude that the fourth or higher layers below the surface do not significantly influence the surface stresses. It also implies that the stress field of the individual

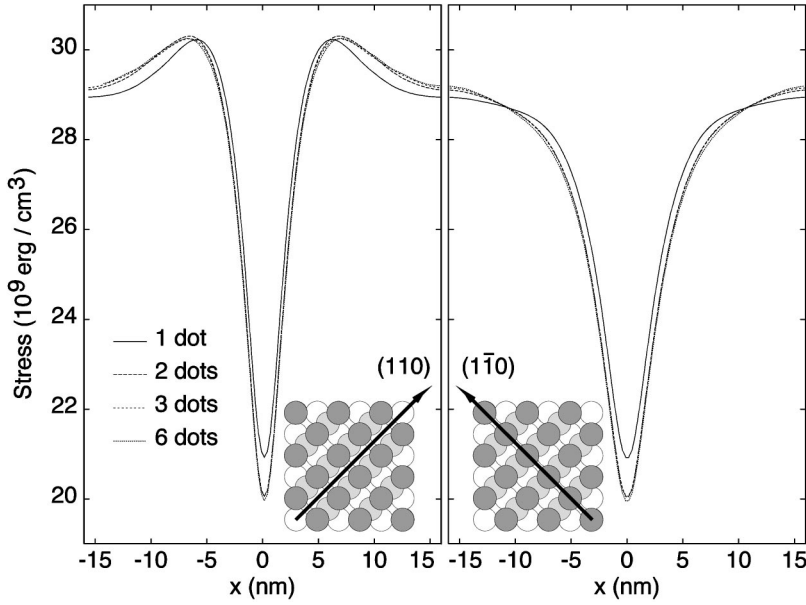


FIG. 3. Surface stress σ along the (110) and $(1\bar{1}0)$ directions for 1, 2, 3, and 6 quantum dot layers.

dots decays rapidly, in particular a comparison of the different curves implies an approximate r^{-3} decay. This fast decay also accounts for the result that the elastic stress distribution on the surface is almost the same for the one, two, and three dot layer systems, a result which has an important consequence on island nucleation. Namely, the preferred nucleation sites will lie directly above centers of the uppermost capped dots, provided that the vertical separation between consecutive island layers is small. As this vertical separation between dot layers is increased, the fast decay of the dot-induced stress field means that the stress minima on the surface will become less pronounced, so that islands may begin to nucleate elsewhere, and not necessarily above the underlying (deeply embedded) dots.

The nucleation properties of the dots are primarily governed by the elastic stress distribution on the surface, so that in addition to the accurate results obtained by our MD simulations, it is also of great importance to determine how well the stress fields can be approximated by simple analytic models. Using linear elasticity theory, Ref. 6 considered pointlike islands, or equivalently force dipoles, to model the stress distribution in two dimensions. In the following, we try to approximate the surface stress field of a single embedded quantum dot layer by that of a corresponding force dipole layer.

The stress field [$\sigma^{fd}(x,y,L) = \sigma_{xx}^{fd} + \sigma_{yy}^{fd}$] on the surface induced by a force-dipole buried at $x=0, y=0, z=-z_0$ in three dimensions is given by²²

$$\sigma^{fd} = \frac{P}{R^3} \left\{ 1 - \frac{3}{R^2} \left[\frac{4-4\nu}{4-8\nu} (x^2+y^2) - \frac{8\nu z_0^2}{4-8\nu} \right] \right\}, \quad (2)$$

where P is the strength of the dipole, (x,y) denotes the position on the surface, $R = (x^2 + y^2 + z_0^2)^{1/2}$, and $\nu = 0.218$ is Poisson's ratio for the Si embedding matrix.

To calculate the stress field distribution on the surface we have to sum up the contribution of Eq. (2) over all the buried force-dipoles that form a two dimensional square lattice with lattice constant L , i.e.,

$$\sigma_{tot}^{fd}(x,y) = \sum_{i=-\infty}^{+\infty} \sum_{j=-\infty}^{+\infty} \sigma^{fd}(x-iL, y-jL, z_0) + \sigma_{tot}^0. \quad (3)$$

The term σ_{tot}^0 accounts for the homogeneous misfit stress present in the compressed Ge surface layer.

Since σ^{fd} is radially symmetric, we compare $\sigma_{tot}^{fd}(x,x)$ to our MD stresses averaged for the (110) and $(1\bar{1}0)$ directions, i.e., we try to find the best agreement between $\sigma_{tot}^{fd}(x,x)$ and

$$\begin{aligned} \sigma_{tot}^{MD}(x,x) = & 1/2 \{ \sigma_{xx}^{MD}(x,x) + \sigma_{xx}^{MD}(x,-x) \\ & + \sigma_{yy}^{MD}(x,x) + \sigma_{yy}^{MD}(x,-x) \}. \end{aligned}$$

Equation (3) contains three unknown parameters: σ_{tot}^0 , P , and z_0 . We require that $\sigma_{tot}^0 = 28.692 \times 10^9 \text{ erg/cm}^3$, the value found by a MD simulation for a system with no embedded dots. We also require that the averages of σ_{tot}^{fd} and

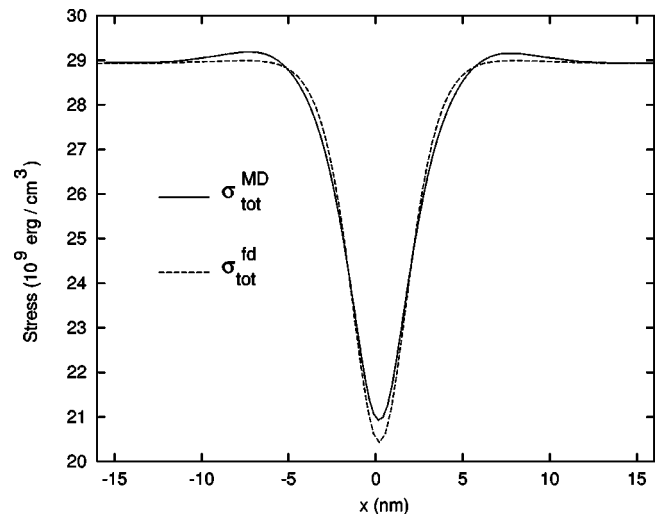


FIG. 4. Comparison between the MD surface stress (σ_{tot}^{MD} , solid line) and the force dipole approximation (σ_{tot}^{fd} , dashed line) for a single embedded quantum dot layer.

σ_{tot}^{MD} are equal, providing a relationship between P and z_0 . Consequently, we are left with a single adjustable parameter z_0 which is varied to fit σ_{tot}^{fd} to the ‘‘experimental’’ σ_{tot}^{MD} curve. The best fit (shown in Fig. 4) was obtained for $z_0 = 1.2H = 5.4$ nm and $P = 1.772 \times 10^{-10}$ erg. It is not surprising that $z_0 > H$ for the optimal fit, since the embedded dots are extended objects that stretch the stress field in both horizontal directions. The fit is quite good, considering that the diamond lattice-induced anisotropy is beyond the scope of this simple force-dipole model.

In summary, by making use of large-scale MD techniques we have determined the stress distribution on the surface for a Ge/Si quantum dot superlattice. Our results demonstrate that the stress is minimal directly above the uppermost buried dot, decaying rapidly (r^{-3}) with the depth of the dot.

This supports the experimental observation that vertical ordering can be dramatically improved by decreasing the capping layer thickness. We also compared the MD stress distribution with the analytic force-dipole solution and found good agreement. Thus, to model the elastic properties of these systems and consequently study the nucleation and ordering properties of the dots, it is sufficient to use the continuum elasticity force-dipole approximation.

The work at Los Alamos was performed under the auspices of the U.S. Department of Energy. We thank the Advanced Computing Laboratory for the use of their SGI Origin 2000s, on which the current simulations were performed. I.D. and A.L.B. were partially supported by ONR YI Award No. N00014-98-1-0575 and by DOE.

-
- ¹S. Rouvimov *et al.*, J. Electron. Mater. **27**, 427 (1998).
²Other stacked quantum dot systems include Ge/Si, A. A. Darhuber *et al.*, Thin Solid Films **294**, 296 (1997); GaN/AlN, F. Widmann *et al.*, J. Appl. Phys. **83**, 7618 (1998); and InP/GaInP, M. K. Zundel *et al.*, Appl. Phys. Lett. **71**, 2972 (1997).
³G. Springholz, V. Holy, M. Pinczolits, and G. Bauer, Science **282**, 734 (1998).
⁴Y. Nakata, Y. Sugiyama, T. Futatsugi, and N. Yokoyama, J. Cryst. Growth **175**, 713 (1997).
⁵G. S. Solomon, S. Komarov, J. S. Harris, and Y. Yamamoto, J. Cryst. Growth **175**, 707 (1997).
⁶J. Tersoff, C. Teichert, and M. G. Lagally, Phys. Rev. Lett. **76**, 1675 (1996).
⁷F. Liu, S. E. Davenport, H. M. Evans, and M. G. Lagally, Phys. Rev. Lett. **82**, 2528 (1999).
⁸S. J. Zhou, D. M. Beazley, P. S. Lomdahl, and B. L. Holian, Phys. Rev. Lett. **78**, 479 (1997).
⁹S. J. Zhou, D. L. Preston, P. S. Lomdahl, and D. M. Beazley, Science **279**, 1525 (1998).
¹⁰B. L. Holian and P. S. Lomdahl, Science **280**, 2085 (1998).
¹¹D. M. Beazley and P. S. Lomdahl, Parallel Computing **20**, 173 (1994).
¹²P. S. Lomdahl, P. Tamayo, N. Grønbech-Jensen, and D. M. Beazley, in *Proceedings of Supercomputing 93* (IEEE Computer Society Press, Los Alamitos, CA, 1993), pp. 520–527.
¹³D. M. Beazley and P. S. Lomdahl, Comput. Phys. **11**(3), 230 (1997).
¹⁴A. A. Darhuber *et al.*, Phys. Rev. B **55**, 15 652 (1997).
¹⁵F. H. Stillinger and T. A. Weber, Phys. Rev. B **31**, 5262 (1985).
¹⁶C. Roland and G. H. Gilmer, Phys. Rev. B **47**, 16 286 (1993).
¹⁷X.-P. Li, G. Chen, P. B. Allen, and J. Q. Broughton, Phys. Rev. B **38**, 3331 (1988).
¹⁸P. C. L. Stephenson, M. W. Radny, and P. V. Smith, Surf. Sci. **366**, 177 (1996).
¹⁹K. E. Khor and S. Das Sarma, Phys. Rev. B **36**, 7733 (1987).
²⁰J. B. Gibson, A. N. Goland, M. Milgram, and G. H. Vineyard, Phys. Rev. **120**, 1229 (1960).
²¹R. J. Hardy, J. Chem. Phys. **76**, 622 (1982).
²²S. M. Hu, J. Appl. Phys. **66**, 2741 (1989).